

Supplemental material for

Comparing malignant monocytosis across the updated WHO and ICC classifications of 2022

Francis Baumgartner^{1,2,3}, Constance Baer^{1#}, Stefanos Bamopoulos^{2,3#}, Edward Ayoub^{1,4}, Marietta Truger¹, Manja Meggendorfer¹, Miriam Lenk¹, Gregor Hoermann¹, Stephan Hutter¹, Heiko Müller¹, Wencke Walter¹, Martha-Lena Müller¹, Niroshan Nadarajah¹, Piers Blombery^{1,5}, Ulrich Keller^{2,6}, Wolfgang Kern¹, Claudia Haferlach¹, Torsten Haferlach^{1,*}

*Corresponding Author. E-mail: torsten.haferlach@mll.com

This PDF file includes:

Supplemental Methods

Figs. S1 to S9

Supplemental References (1. to 14.)

Other Supplemental Materials for this manuscript include the following:

Tables S1 to S8

Supplemental Methods

Flow cytometric analysis. Based on Euroflow Consortium recommendations the stain-lyse-wash procedure with FACS Lysing Solution (BD Biosciences, San Jose, CA) was followed. Twelve cell surface staining of 2×10^6 cells was performed, and at least 5×10^5 total events were acquired per tube (FACS Canto II; BD Biosciences). Analysis was performed with Infinicyt (v1.7, Cytognos SL, Salamanca, Spain). In the absence of specific criteria in the ICC22 classification system and taking into account the well-known parallels of aberrant phenotypes in CMML and MDS, we considered ≥ 3 aberrancies as fulfillment of the “abnormal immunophenotyping consistent with CMML” criterion based on the respective criteria specified for MDS by the ELN working group on flow cytometry in MDS.^{1,2} Aberrant expression of the following surface markers was assessed: (I) Aberrant expression of CD2, CD5, CD7, CD11b, CD15, CD19, CD56 in blasts, CD11b/CD16, CD11b/CD13, CD13/CD16, CD56 in granulocytes, and CD2, CD56 in monocytes. (II) Reduced expression of CD13, CD33, CD34, CD45, CD117, HLA-DR in blasts, CD13, CD33 in granulocytes, and CD11b, CD13, CD14, CD33, CD45, HLA-DR in monocytes. (III) Increased expression of CD34, HLA-DR in blasts. (IV) Additionally, CD71 expression was assessed on erythrocytes. As peripheral blood and bone marrow samples were not available for all samples, aberrant immunophenotypes were considered from either the peripheral blood or the bone marrow, or both.

Definition of pathogenicity and variant allele frequency. Pathogenicity of mutations was assessed based on a 4-tier system, with *Tier1* being clearly pathogenic, *Tier2* possibly pathogenic, *Tier3* variants of unknown significance, and *Tier4* polymorphisms.³ *Tier3* and *Tier4* mutations were excluded from downstream analyses. In the case of serial sequencing results of one patient (defined as less than 4 weeks interval), the higher VAF was used for downstream analyses.

Evidence of clonality was defined as the presence of either (I) a known pathological mutation with a VAF $>2\%$ (WHO22) or a VAF $>10\%$ (ICC22), (II) a karyotypic alteration present in at least 2/20 metaphases, or (III) a cryptical deletion evidenced through FISH analysis. For the assessment of the evidence of clonality criterion only samples with ≥ 10 genes were considered.

WHO 2017.⁴ The classification sequence followed is depicted in Figure S3A. In the case of CMML diagnosis in absence of dysplasia, the criterion of persisting monocytosis >3 months under the exclusion of alternative diagnosis was presumed to have been followed, as only clinical information from selected time points was available per patient. CMML cases were classified as CMML-0 ($<2\%$ blasts in PB and $<5\%$ blasts in BM), CMML-1 (2–4% blasts in PB

and/or 5–9% blasts in BM), and CMML-2 (5–19% blasts in PB, 10–19% in BM, presence of Auer rods).

WHO 2022.⁵ CMML: The classification sequence followed is depicted in Figure S3B. Abnormal partitioning of PB monocyte subsets defined as $\geq 94\%$ classical MO1 monocytes was not routinely assessed before 2022 but has been reviewed extensively elsewhere.^{6,7} The criterion was excluded from the automatized classification process, reducing the CMML_{est} cohort by approximately 100 CMML cases without concurrent dysplasia or clonality. MDS: The MDS-biTP53 subgroup was defined by a Tp53 mutation with VAF $\geq 55\%$, 2 different Tp53 mutations with VAF $\geq 2\%$, and karyotypical chr17 loss or 17p deletion additional to one Tp53 mutation. Copy number neutral loss of heterozygosity (CNN-LOH) data was not routinely assessed in the analyzed patient cohort. MDS-f: No histological results were available for the included cases, leading us to disregard the MDS-f category from the reclassification process.

ICC 2022.⁸ The classification sequence followed is depicted in Figure S3C. ICC22 CMML BM morphology was defined as an age-adjusted hypercellular BM. Abnormal immunophenotyping consistent with CMML was defined as ≥ 3 of the aforementioned, aberrant flow cytometric findings. i17q CMML cases present overlap with the MDS/MPN i17q category, which was disregarded in all downstream analyses.

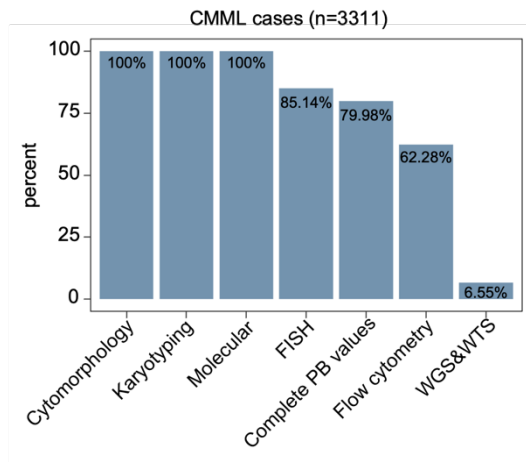
Differential gene expression analysis. The count matrix was normalized with edgeR (v3.32.1).⁹ Genes with low expression were removed via the filterByExpr function. Afterward TMM- and library size normalization was performed with calcNormFactors. Differential gene expression was called with the lmFit, contrast.fit, and eBayes functions of the limma package (v3.46.0). after sample-weighting with voomWithQualityWeights.^{10–12} The percentage of monocytes in the bone marrow was included as a cofactor when estimating differential gene expression to limit bias due to different BM compositions.

Gene Set Enrichment Analysis (GSEA). GSEA was performed using the fgsea (v.1.16.0) package. Genes were ranked according to the logFC as a measure of differential expression. The fgsea function was run using default parameters for the hallmark gene sets defined in the Molecular Signatures Database v7.4.^{13,14} The ClusterProfiler and enrichplot packages were used for visualization purposes.

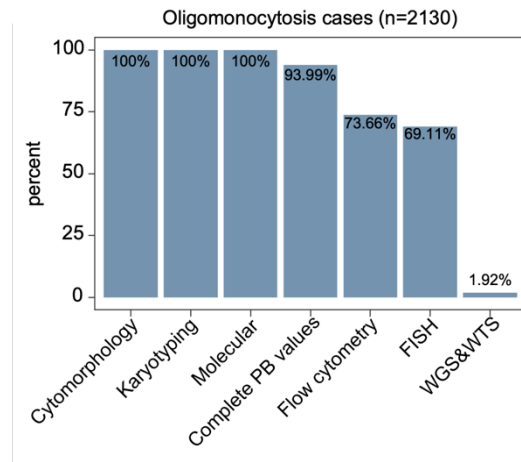
Supplemental Figures and Legends

fig. S1

A



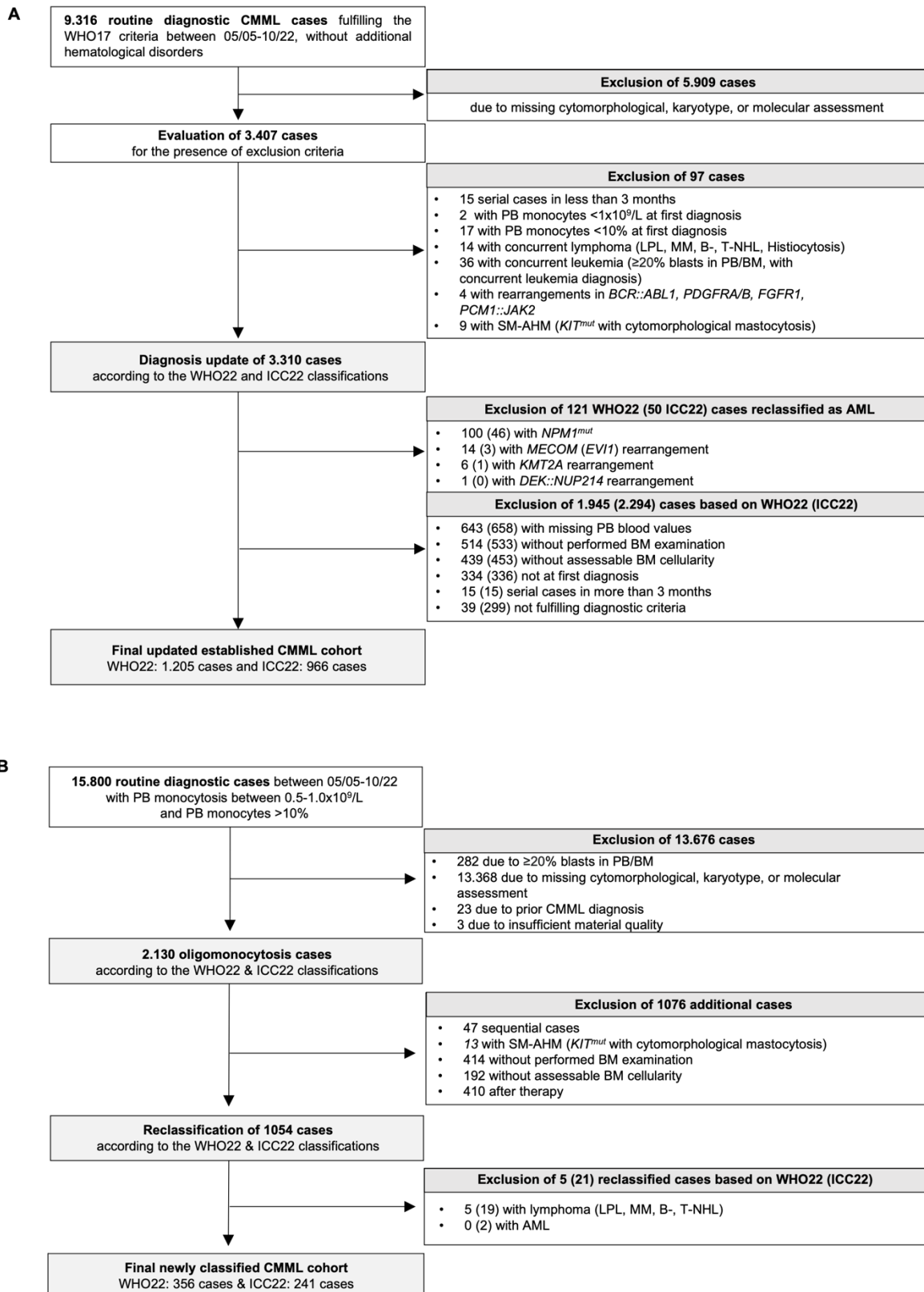
B



Supplemental Figure S1. Summary of the different analyses performed. **(A)** Analyses performed for the 3,311 established CMML cases. **(B)** Analyses performed for the 2,130 oligomonocytosis cases.

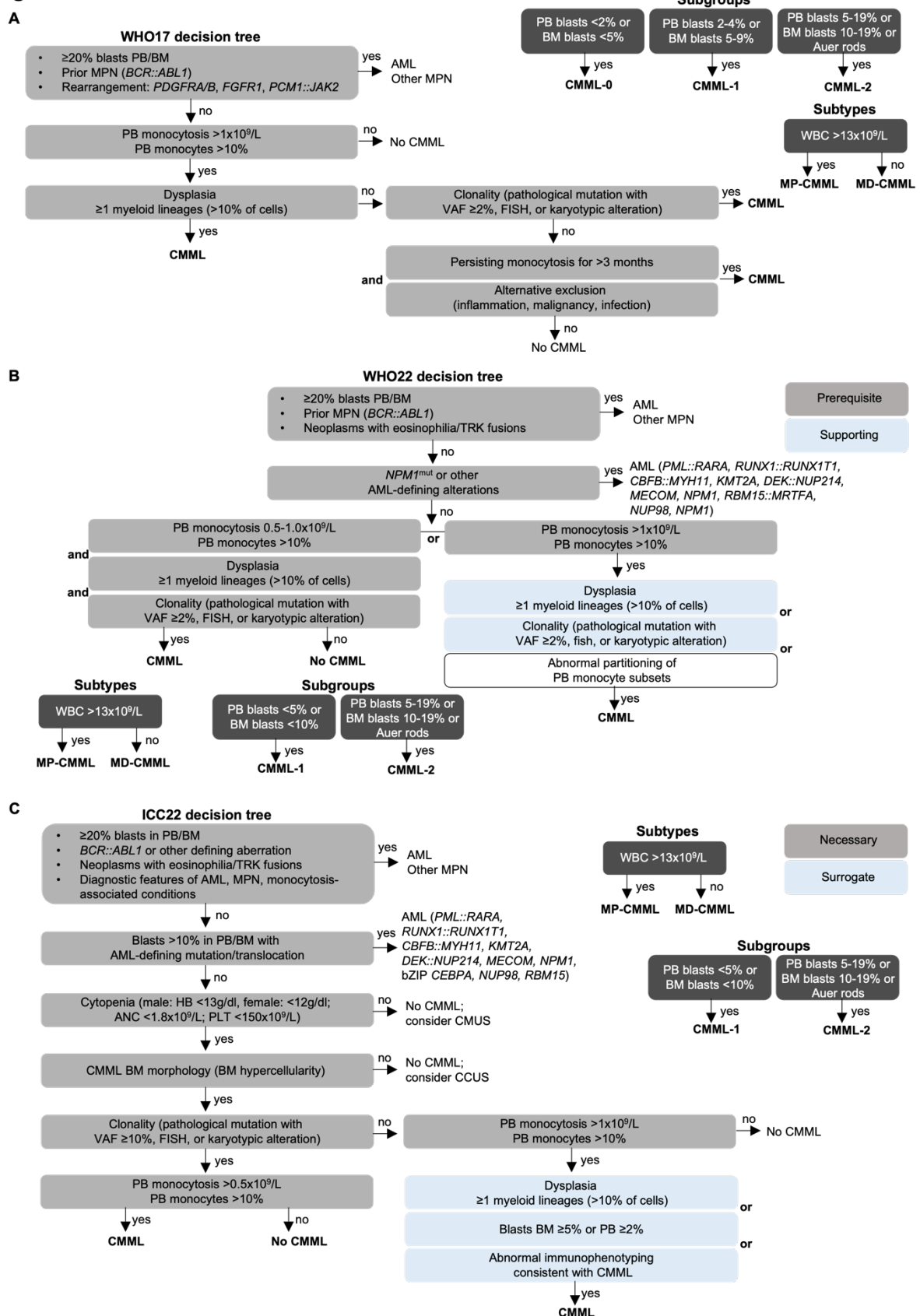
PB: Peripheral Blood, WGS: Whole Genome Sequencing, WTS: Whole Transcriptome Sequencing.

fig. S2



Supplemental Figure S2. Filtering process applied to define the final cohorts used for downstream analyses. **(A)** Established CMML cases. **(B)** Oligomonocytosis cases.

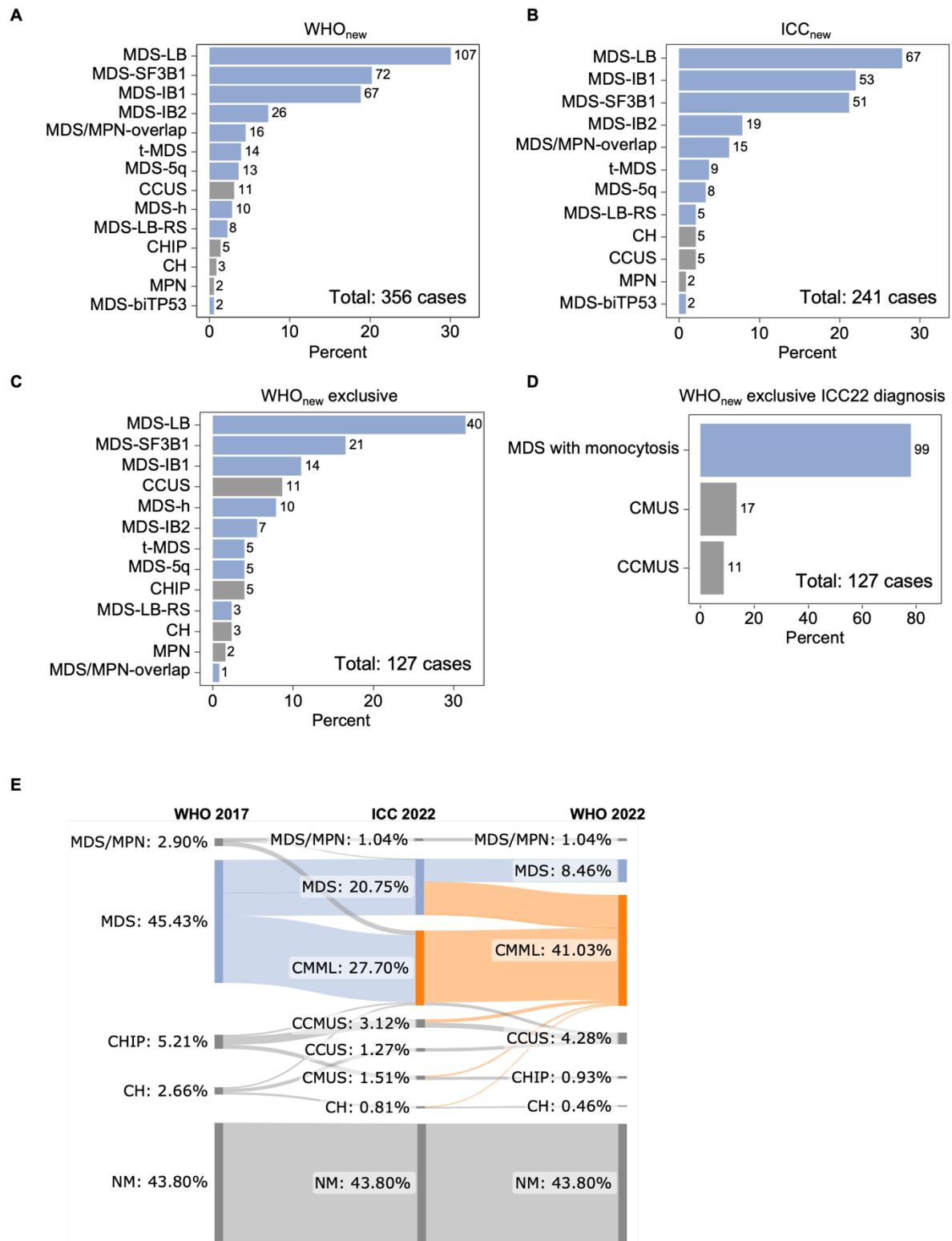
fig. S3



Supplemental Figure S3. Classification sequences applied for patient classification. **(A)** WHO 2017 classification. **(B)** WHO 2022 classification. Of note, the criterion “abnormal

partitioning of PB monocyte subsets” was not routinely assessed before 2022 and was thus excluded from the analysis. **(C)** ICC 2022 classification.

fig. S4



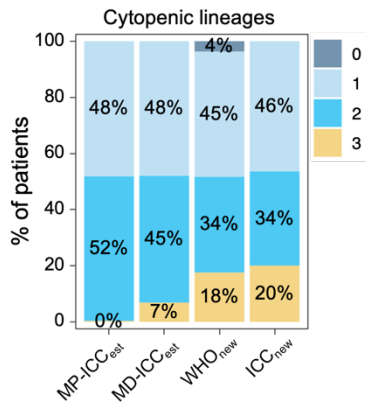
Supplemental Figure S4. (A-C) Prior diagnoses updated to their WHO22 equivalent of the **(A)** 356 WHO_{new} cases. **(B)** 241 ICC_{new} cases. **(C)** 127 WHO_{new} exclusive cases. **(D)** Respective ICC22 diagnoses of the 127 WHO_{new} exclusive cases **(E)** Diagnosis update of 863 well-described monocytosis cases (absolute monocyte count of $0.5-1 \times 10^9/L$ and higher 10%, no prior CMML diagnosis) after exclusion of lymphoma, AML, and ALL cases from the WHO17

to the ICC22, and the WHO22 classifications. Specific focus was put onto the premalignant monocytosis categories of CH/CHIP (WHO17), CH/CCUS/CMUS/CCMUS (ICC22), and CH/CHIP/CCUS (WHO22).

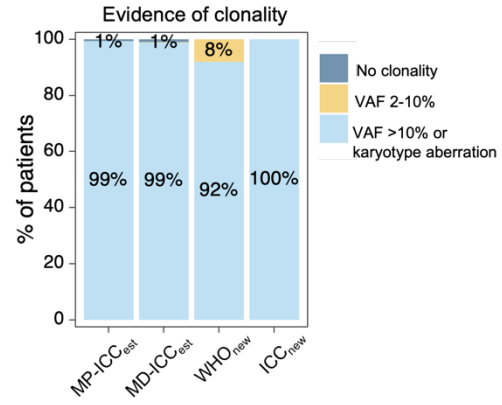
CH: Clonal hematopoiesis, CHIP: Clonal Hematopoiesis of Indeterminate Potential, CCUS: Clonal Cytopenia of Unknown Significance, CMUS: Clonal Monocytosis of Unknown Significance, CCMUS: Clonal Cytopenia and Monocytosis of Unknown Significance, IB: Intermediate blasts, LB: Low blasts, MDS: Myelodysplastic Neoplasia, MPN: Myeloproliferative Neoplasia, NM: Non-malignant, t-MDS: therapy-related MDS.

fig. S5

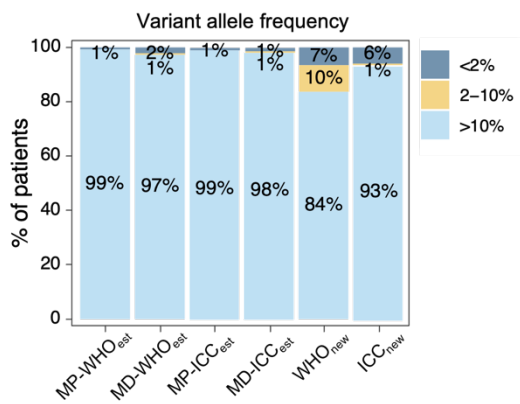
A



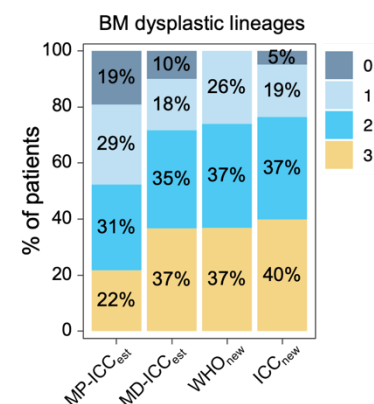
B



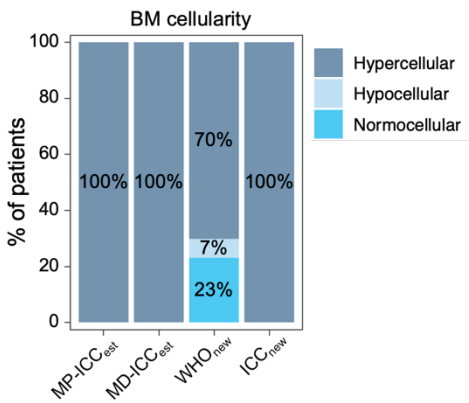
C



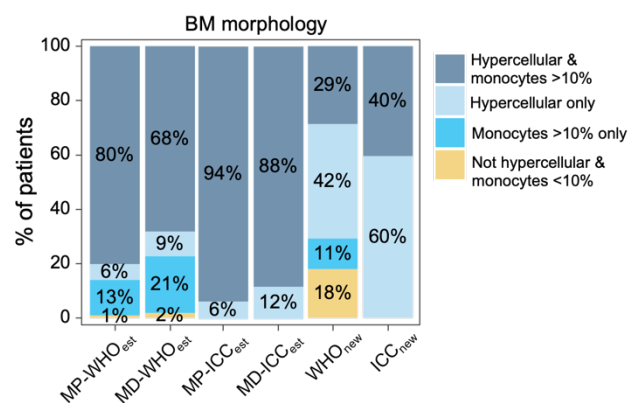
D



E

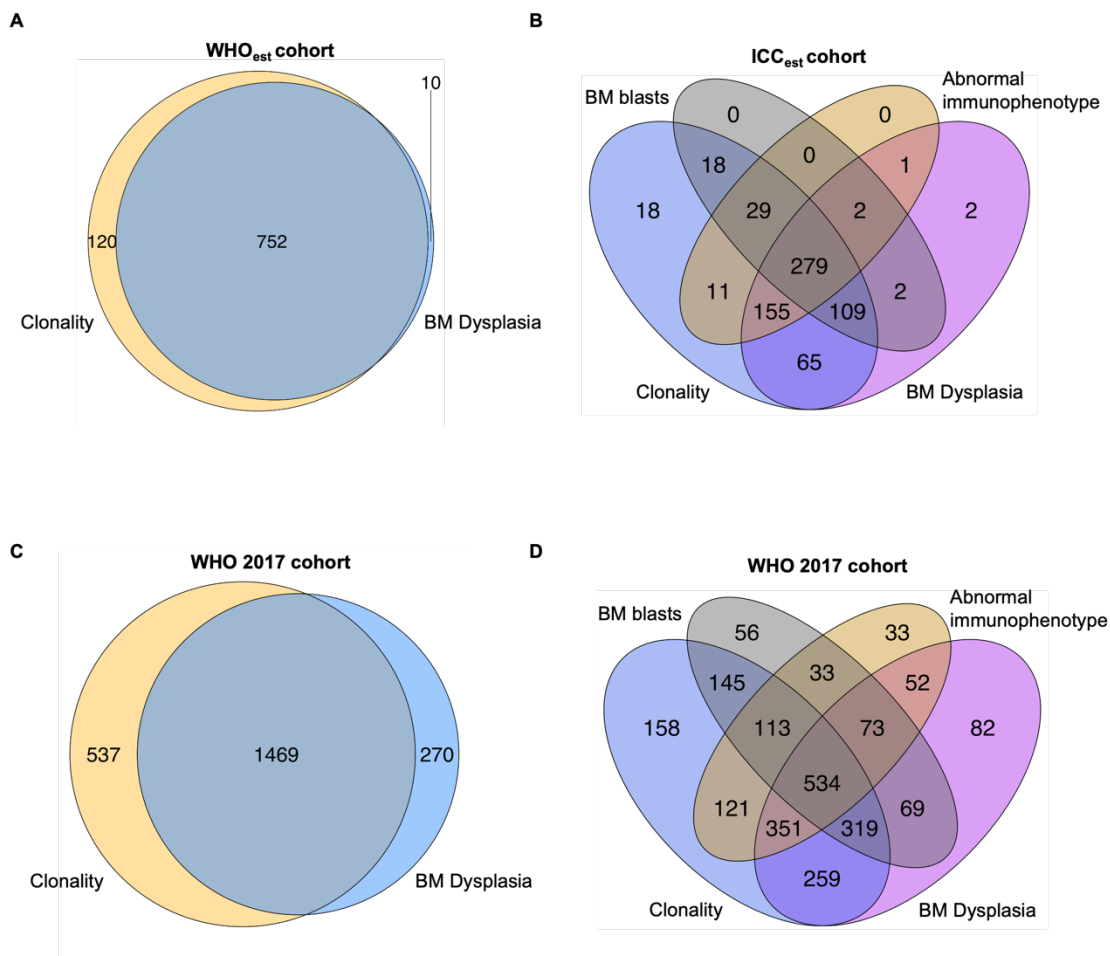


F



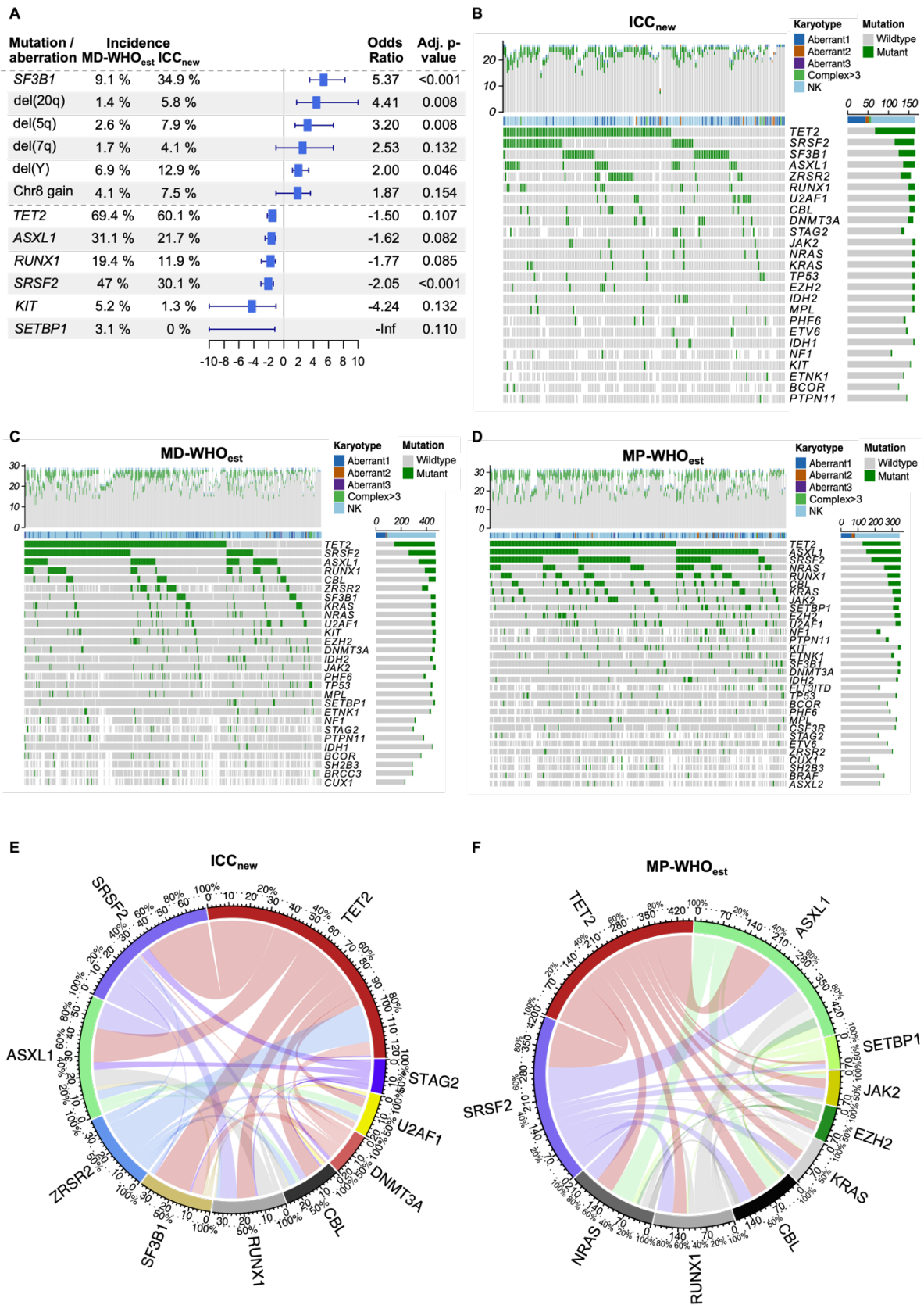
Supplemental Figure S5. Classification criteria analysis in the ICC_{est} and WHO_{est} (both subdivided into MD-CMML and MP-CMML), WHO_{new} and ICC_{new} cohorts. **(A)** Number of cytopenic lineages in the peripheral blood. **(B)** Evidence of clonality in patients with ≥ 10 genes sequenced. Patients were separated into “no clonality” (maximal VAF of myeloid malignancy associated mutations $< 2\%$), VAF between 2-10%, and VAF $> 10\%$ or karyotypical alteration. **(C)** Variant allele frequency. **(D)** Number of dysplastic lineages in the BM. **(E)** Age-adjusted BM cellularity. **(F)** Presence of hypercellularity and monocytosis (defined as $> 10\%$ monocytes) in the BM.

fig. S6



Supplemental Figure S6. (A) Overlap between the diagnostic criteria of clonality and BM dysplasia in 882 WHO_{est} cases with ≥ 10 genes sequenced. **(B)** Overlap between the diagnostic criteria of clonality, BM dysplasia, BM blasts, and ICC22 abnormal immunophenotyping in the 691 cases of the ICC_{est} cohort with ≥ 10 genes sequenced. **(C)** Overlap between the diagnostic criteria of clonality and BM dysplasia in 2455 established CMML cases as defined by the WHO17 classification. **(D)** Overlap between the diagnostic criteria of clonality, BM dysplasia, BM blasts, and ICC22 abnormal immunophenotyping in 2455 established CMML cases as defined by the WHO17 classification.

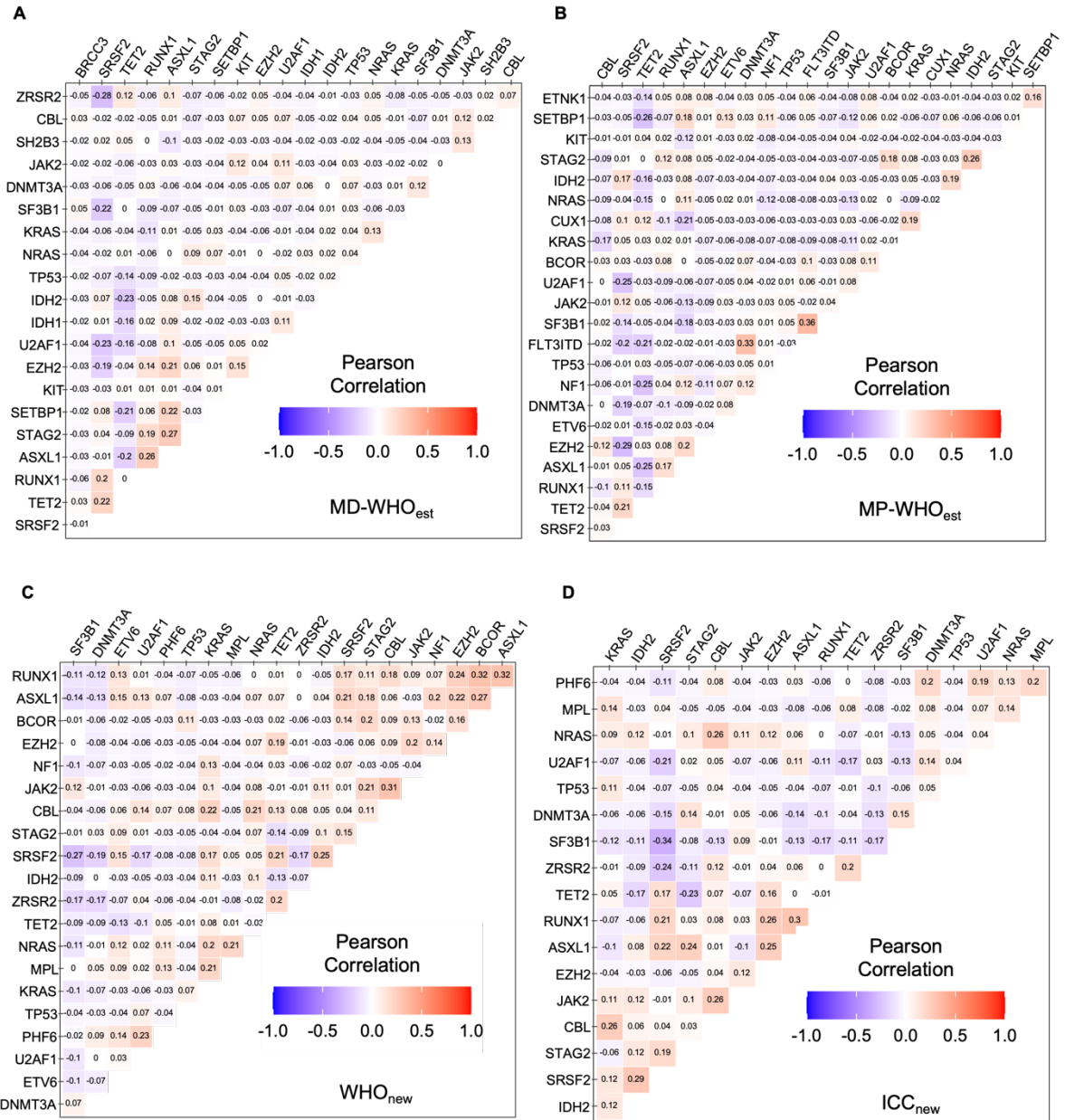
fig. S7



Supplemental Figure S7. (A) Forest Plot comparing the incidences and odds ratios of 12 alterations significantly differing between 654 MD-WHO_{est} and 241 ICC_{new} cases. **(B-D)**

Oncoprints depicting the 24 mutations with highest incidence and respective karyotypes, ordered from the most to the least frequently mutated, with each column representing a patient and each row representing a gene. Number of mutations identified/genes assessed by NGS per patient is shown as columns in the top row. Mutations were identified in **(B)** 164 ICC_{new}, **(C)** 474 MD-WHO_{est} and **(D)** 351 MP-WHO_{est} cases with >20 genes sequenced. **(E-F)** Circos plots showing the co-mutational profile in **(E)** 164 ICC_{new} and **(F)** 351 MP-WHO_{est} cases with >20 genes sequenced.

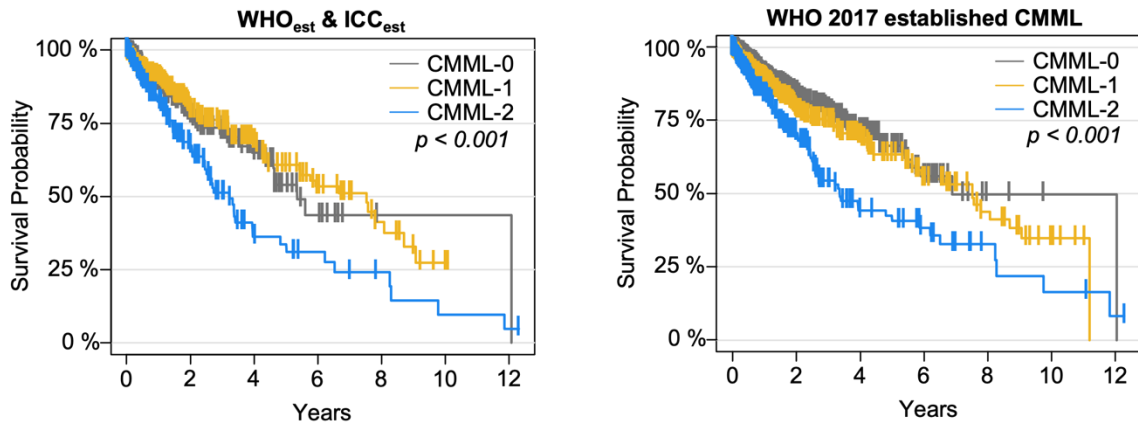
fig. S8



Supplemental Figure S8. (A-D) Correlation matrices depicting genes frequently co-mutated in the same patient in red, and genes with lower co-mutational frequency than expected in blue. Depicted are the results from **(A)** 654 MD-WHO_{est}, **(B)** 551 MP-WHO_{est}, **(C)** 356 WHO_{new}, **(D)** 241 ICC_{new} cases.

fig. S9

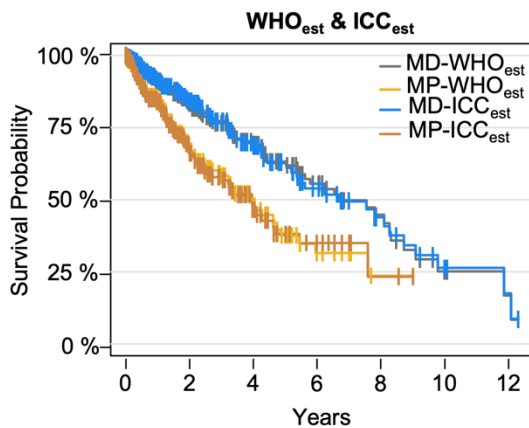
A



CMML-0	465	78	30	8	1	1	1
CMML-1	492	106	55	26	11	3	0
CMML-2	281	55	15	9	5	2	1

CMML-0	1057	170	67	19	3	1	1
CMML-1	820	157	75	35	17	7	0
CMML-2	524	82	27	15	6	3	1

B



MD-WHO _{est}	654	137	66	33	15	6	2
MP-WHO _{est}	551	96	32	9	2	0	0
MD-ICC _{est}	496	109	55	27	14	6	2
MP-ICC _{est}	470	81	26	9	2	0	0

Supplemental Figure S9. (A-C) Kaplan-Meier-Curves comparing the **(A)** merged WHO_{est} and ICC_{est} cohorts used for comparison throughout this study (left) and all established CMML cases at first diagnosis (right). These were divided into the CMML-0, CMML-1, and CMML-2 groups, as defined by the WHO 2017 classification. CMML-0 showed a median OS of 5.4 (6.9) years, vs. 7.5 (7.5) years in CMML-1, and 3.4 (3.2) years in CMML-2. **(B)** WHO_{est} and ICC_{est} cohorts divided into MD- and MP-CMML groups. MD-WHO_{est} and MD-ICC_{est} showed a median OS of 6.7 (6.7) years, vs. 4 (3.9) years in MP-WHO_{est} and MP-ICC_{est}.

Supplemental References

1. Westers TM, Ireland R, Kern W, et al. Standardization of flow cytometry in myelodysplastic syndromes: a report from an international consortium and the European LeukemiaNet Working Group. *Leukemia*. 2012;26(7):1730–1741.
2. Porwit A, van de Loosdrecht AA, Bettelheim P, et al. Revisiting guidelines for integration of flow cytometry results in the WHO classification of myelodysplastic syndromes—proposal from the International/European LeukemiaNet Working Group for Flow Cytometry in MDS. *Leukemia*. 2014;28(9):1793–1798.
3. Li MM, Datto M, Duncavage EJ, et al. Standards and Guidelines for the Interpretation and Reporting of Sequence Variants in Cancer. *J. Mol. Diagn. JMD*. 2017;19(1):4–23.
4. Arber DA, Orazi A, Hasserjian R, et al. The 2016 revision to the World Health Organization classification of myeloid neoplasms and acute leukemia. *Blood*. 2016;127(20):2391–2405.
5. Khoury JD, Solary E, Abla O, et al. The 5th edition of the World Health Organization Classification of Haematolymphoid Tumours: Myeloid and Histiocytic/Dendritic Neoplasms. *Leukemia*. 2022;36(7):1703.
6. Selimoglu-Buet D, Myélodysplasies on behalf of the GF des, Badaoui B, et al. Accumulation of classical monocytes defines a subgroup of MDS that frequently evolves into CMML. *Blood*. 2017;130(6):832–835.
7. Selimoglu-Buet D, Myélodysplasies on behalf of the GF des, Wagner-Ballon O, et al. Characteristic repartition of monocyte subsets as a diagnostic signature of chronic myelomonocytic leukemia. *Blood*. 2015;125(23):3618–3626.
8. Arber DA, Orazi A, Hasserjian RP, et al. International Consensus Classification of Myeloid Neoplasms and Acute Leukemia: Integrating Morphological, Clinical, and Genomic Data. *Blood*. 2022;
9. Gierliński M, Cole C, Schofield P, et al. Statistical models for RNA-seq data derived from a two-condition 48-replicate experiment. *Bioinformatics*. 2015;31(22):3625.
10. Law CW, Chen Y, Shi W, Smyth GK. voom: precision weights unlock linear model analysis tools for RNA-seq read counts. *Genome Biol*. 2014;15(2):R29.
11. Liu R, Holik AZ, Su S, et al. Why weight? Modelling sample and observational level variability improves power in RNA-seq analyses. *Nucleic Acids Res*. 2015;43(15):e97.
12. Ritchie ME, Phipson B, Wu D, et al. limma powers differential expression analyses for RNA-sequencing and microarray studies. *Nucleic Acids Res*. 2015;43(7):e47.
13. Liberzon A, Birger C, Thorvaldsdóttir H, et al. The Molecular Signatures Database (MSigDB) hallmark gene set collection. *Cell Syst*. 2015;1(6):417.
14. Subramanian A, Tamayo P, Mootha VK, et al. From the Cover: Gene set enrichment analysis: A knowledge-based approach for interpreting genome-wide expression profiles. *Proc. Natl. Acad. Sci. U. S. A*. 2005;102(43):15545.

Data (separate files)

Table S1: ICC22 and WHO22 reclassified established CMML and oligomonocytosis cases.

Table S2.1: Clinicopathological parameters in WHO_{est} and ICC_{est} cases.

Table S2.2: Immunophenotypes in WHO_{est} and ICC_{est} cases.

Table S2.3: Cytogenetic alterations in WHO_{est} and ICC_{est} cases.

Table S2.4: Mutational profiles and FISH alterations in WHO_{est} and ICC_{est} cases.

Table S3: IPSS-M scoring results in WHO_{new} and ICC_{new} cases.

Table S4: DEG of MP-WHO_{est} vs. controls

Table S5: DEG of MD-WHO_{est} vs. controls

Table S6: DEG of WHO_{new} vs. controls

Table S7: DEG of WHO_{new} vs. MD-WHO_{est}

Table S8: GSEA of hallmark genesets of WHO_{new} vs. MD-WHO_{est}